Structural Engineering and Mechanics, Vol. 42, No. 1 (2012) 55-72
DOI: http://dx.doi.org/10.12989/sem.2012.42.1.055

Modelling and integrity assessment of shear connectors in precast cast-in-situ concrete bridges

Pilate Moyo*, Bongani Sibanda and Hans Beushausen

Department of Civil Engineering, University of Cape Town, Cape Town, South Africa

(Received July 15, 2011, Revised February 15, 2012, Accepted February 28, 2012)

Abstract. Precast-cast insitu concrete bridge construction is widely practiced for small to medium span structures. These bridges consist of precast pre-stressed concrete beams of various cross-sections with a cast in-situ reinforced concrete slab. The connection between the beams and the slab is via shear links often included during the manufacturing process of the beams. This form of construction is attractive as it provides for standardisation, reduced formwork and construction time. The assessment of the integrity of shear connectors in existing bridges is a major challenge. A procedure for assessment of shear connectors based on vibration testing and finite element model updating is proposed. The technique is applied successfully to a scaled model bridge model and an existing bridge structure.

Keywords: shear connectors; structural integrity assessment; composite structures; vibration testing; partial composite action

1. Introduction

The development of pre-cast prestressed concrete beams for bridge construction started around 1948 in Europe with the introduction of the so called WR section (Taylor 1998). Since then a number of cross-sections have been developed and used for bridge construction (Fig. 1). These beams are popular for bridge construction as they offer reduced time of construction and ease of construction for a number of structural forms including simply supported bridges, continuous bridges and integral bridges. Typically these bridges consist of pre-cast beams pre-tensioned concrete beams and cast in-situ concrete slabs. The slab is connected to the beams using stir-ups cast into the beams. Fig. 2 shows a typical connection detail of a concrete-concrete composite bridge.

A number of such bridges have been in operation for more than 30 years and some are showing signs of distress. One of the main challenges in condition assessment of these bridges is the assessment of the integrity of the connection between the beams and the cast in-situ slab owing to accessibility difficulties. A sound understanding of the condition and behaviour of the shear connectors is essential for accurate structural evaluation of the bridge structures. The usual approach in structural modelling of these bridges is to assume full composite action between concrete components, that is, the connection between the concrete beam and the concrete slab is assumed to

*Corresponding author, Associate Professor, E-mail: Pilate.Moyo@uct.ac.za

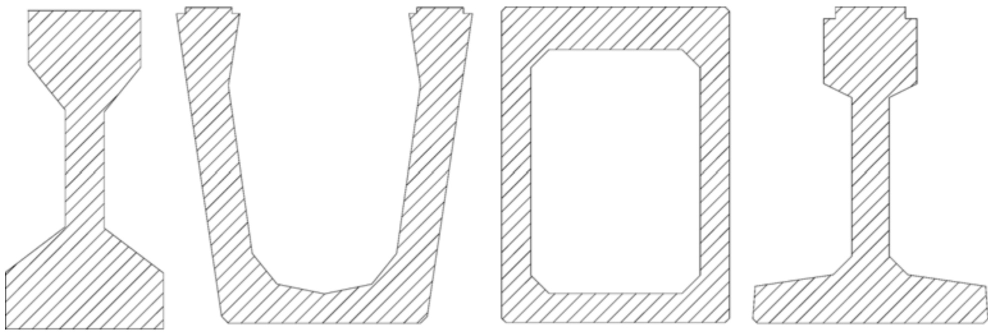

Fig. 1 Typical beam sections

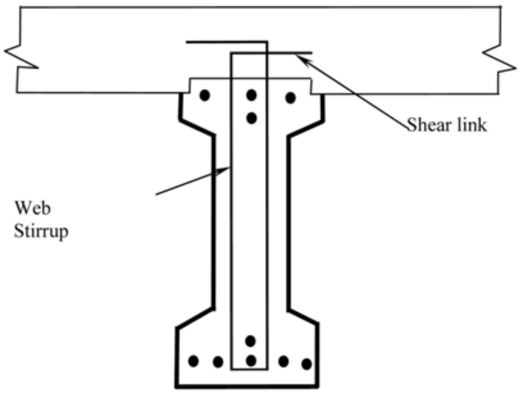

Fig. 2 Beam-slab connection detail for concrete-concrete composite construction

be infinitely rigid. Following work on steel-concrete composites (Wang 1998, Faella *et al.* 2002, Queiroz *et al.* 2007) full composite action is difficult to achieve in normal construction. In this work it is postulated that full composite action between pre-cast prestressed beams and the cast in-situ slab in bridge construction is generally not achieved. Thus the condition assessment of such bridges should include the evaluation of the degree of connectivity between the concrete beams and the slab in order to obtain an accurate bridge structural model. The approach adopted here for assessment of the degree of connectivity between concrete beams and cast in-situ slab is based on numerical models proposed for steel-concrete composites. A review of models used for modelling composite action between steel beams and concrete slabs now follows.

2. Numerical modelling

There is limited technical literature on the behaviour and analysis of the composite action in concrete-concrete composite construction. However there is a substantial body of literature dealing with the behaviour and analysis of steel-concrete composites (Wang 1998, Faella *et al.* 2002, Faella 2003, Clubley *et al.* 2003, Queiroz 2007, Baskar *et al.* 2002, Fu and Lu 2003, Wang 2011, Smitha *et al.* 2011). It is generally accepted that full shear connection between composite components is not easily to achieve and most structures exhibit partial shear interaction, that is, there is relative slip

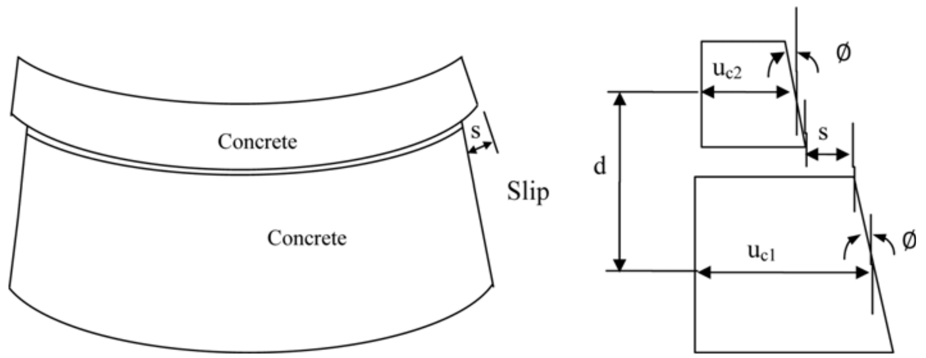

Fig. 3 Partial composite action

between components under load as illustrated in Fig. 3. The interface slip may be expressed as follows

$$s = u_{c1} - u_{c2} - \phi d \tag{1}$$

d = distance between centroids of concrete components.

Partial shear interaction leads to reduced flexural strength and increased deflections compared to structures with full shear interaction (Johnson 1994). The increase in deflections depends on the degree of shear interaction, which in turn depends on the bond strength and the number of shear connectors (Faella 2003). Wright (1990) observed deflection increases of up to 30% for steel-concrete beams with partial shear interaction compared to beams with full shear interaction. It should be noted that that the deflections of concrete structures would also be influenced by the presence of flexural cracks. Owing to the difference in material properties of pre-cast beams and cast in situ concrete, it is reasonable to assume that the behaviour of these composites will be similar to that of steel-concrete composites. Therefore the assumption of full shear interaction would under estimate the deflections of concrete-concrete composites leading to incorrect diagnosis and inappropriate maintenance interventions.

A number of approaches have been proposed for modelling the interaction between steel-concrete composite beams. Fu and Lu (2003) modelled the shear connectors using spring elements with an axial stiffness k_n parallel to the longitudinal axis of the connector and stiffness in the tangential k_t perpendicular to the axis of the connector. The axial stiffness was estimated using

$$k_n = \frac{E_s A_s}{h_s} \tag{2}$$

where E_s = Young's modulus of the shear connector, A_s = area of cross-section of each shear connector, and h_s = height of shear connector.

The stiffness in the tangential direction was modelled using a nonlinear function given

$$k_t = \frac{dP}{ds} = abe^{-bs} \tag{3}$$

P = load and s = interface slip, a and b are constants which depend on the load and slip as follows

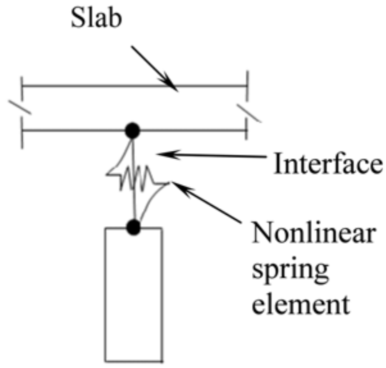

Fig. 4 Partial composite action connection

$$a = \frac{P_1^2}{2P_1 - P_2} \quad \text{and} \quad b = \frac{1}{s_1}\ln\left(\frac{P_1}{P_2 - P_1}\right) \tag{4}$$

The values of P_1 and P_2 are obtained from P versus s curve by choosing two points such that $s_2 = 2s_1$.

Faella *et al.* (2003) proposed the following nonlinear model for estimating the stiffness in the tangential direction

$$k_t = \frac{P_{\max}(1 - e^{\beta s})^{\alpha}}{s} \tag{4}$$

where $P_{\max}$ = the shear connector strength, α and β are constants, and s is local slip. $P_{\max}$, α and β are obtained from pullout tests.

Queiroz *et al.* (2007) used non-linear spring elements to model steel-concrete composite shear connectors (Fig. 4). The stiffness of the springs was estimated from load-slip curves obtained from pullout tests. These springs had, rotational, axial and tangential stiffness and consequently accounted for the shear forces, friction and axial forces in the shear connectors. Wang and Chung (2008) and Macorini *et al.* (2005) also used nonlinear spring elements to simulate shear connectors in a composite steel beam and concrete slab. Both horizontal and vertical springs were used to simulate shear, friction and axial deformation respectively. The stiffness of the springs was estimated using data from pull-out tests.

Delina and Morrassi (2009) estimated the stud tangential stiffness from pull-out tests at 30% of the ultimate shear resistance of the connectors and the axial stiffness was estimated using

$$k_n = \frac{10}{7}\left(\frac{E_s A_s}{e}\right) \tag{5}$$

E_s = Young's modulus of the shear connector, A_s = cross-sectional area of the shear connector, e is the height of the shear connector to the centroid of the concrete slab.

Another approach for modelling the composite action between the slab and beams is through use of smeared contact elements. These elements are capable of modelling the normal stiffness and tangential resistance to shear forces and therefore simulate the interface over an area (Clubley *et al.* 2003). The contact area is allocated stiffness properties for normal and tangential displacements.

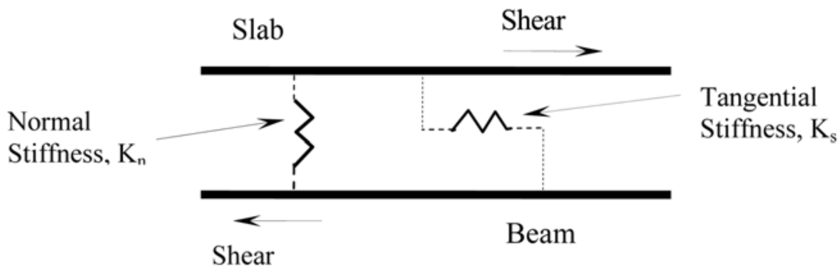

Fig. 5 Smeared element analogy

Clubley *et al.* (2003) stated that these elements have an advantage because they remain a continuum which is subject to variation in stiffness so that further mesh refinement to produce an optimum surface topology is not required. Fig. 5 illustrates a smeared element which is analogous to a spring. However, Clubley *et al.* (2003) noted that it was difficult to achieve acceptable accuracy with smeared interfaces. Clubley *et al.* (2003) observed that use of these elements over the whole shear connector surface resulted in a stiffer model.

Following the review of numerical modelling procedures of steel-concrete composites, there is consensus that:

(i) The shear connector load-slip relation is generally nonlinear. Although attempts have been made to develop mathematical expressions for tangential shear connector stiffness, it is rather difficult to define a universal model. The best approach for estimating the tangential stiffness is by use of load-slip curves obtained from pull-out tests. Johnson and May (1975) suggested estimating the tangential stiffness as the secant stiffness at half the shear connector ultimate load. Wang (1998) proposed the secant stiffness at 80% of the shear connector ultimate load with an equivalent slip of 0.8 mm while Nie *et al.* (2006) used secant stiffness at 66% ultimate load of the shear connectors.

(ii) The axial stiffness of the shear connector takes the form $k_n = \alpha(EA/h)$, where α is constant of proportionality, E is the Young's modulus, A is the cross-sectional area of the shear connector and h is proportional to the height of the shear connector.

In this study the behaviour of concrete composite bridges is investigated through vibrations based testing. The aim is to propose a practical approach for condition assessment of the degree of composite action and hence obtain a representative structural model for determining internal forces and deflections of the concrete hybrid bridges. The investigation involved both laboratory tests on a laboratory bridge model and field tests on an existing concrete composite bridge.

3. Vibration testing

Vibration testing was chosen due to its ability to detect changes in structural behaviour resulting from the introduction of structural damage. Change in structural behaviour is characterised through global vibration characteristics such as natural frequencies, mode shapes and modal assurance criterion (MAC) or local vibration methods such as the coordinate modal assurance criterion (COMAC), the change in mode shape curvature method change in flexibility method, change in stiffness method, change in strain method and the frequency response correlation approach proposed by Xia *et al.* (2007). Global methods provide information about the overall behaviour of the structure while local methods provide information about localised behaviour. This study is focused on global behaviour of concrete-concrete composite structures. While damage localisation in shear connectors is desirable and important, a lot of effort is required to do this using vibration based testing (Xia *et al.* 2007, Xia *et al.* 2008) owing to difficulties in accessing the interface between concrete elements. Where it is necessary to localise shear connector damage, it is proposed to explore non-destructive testing techniques. Thus damage localisation will not be considered here.

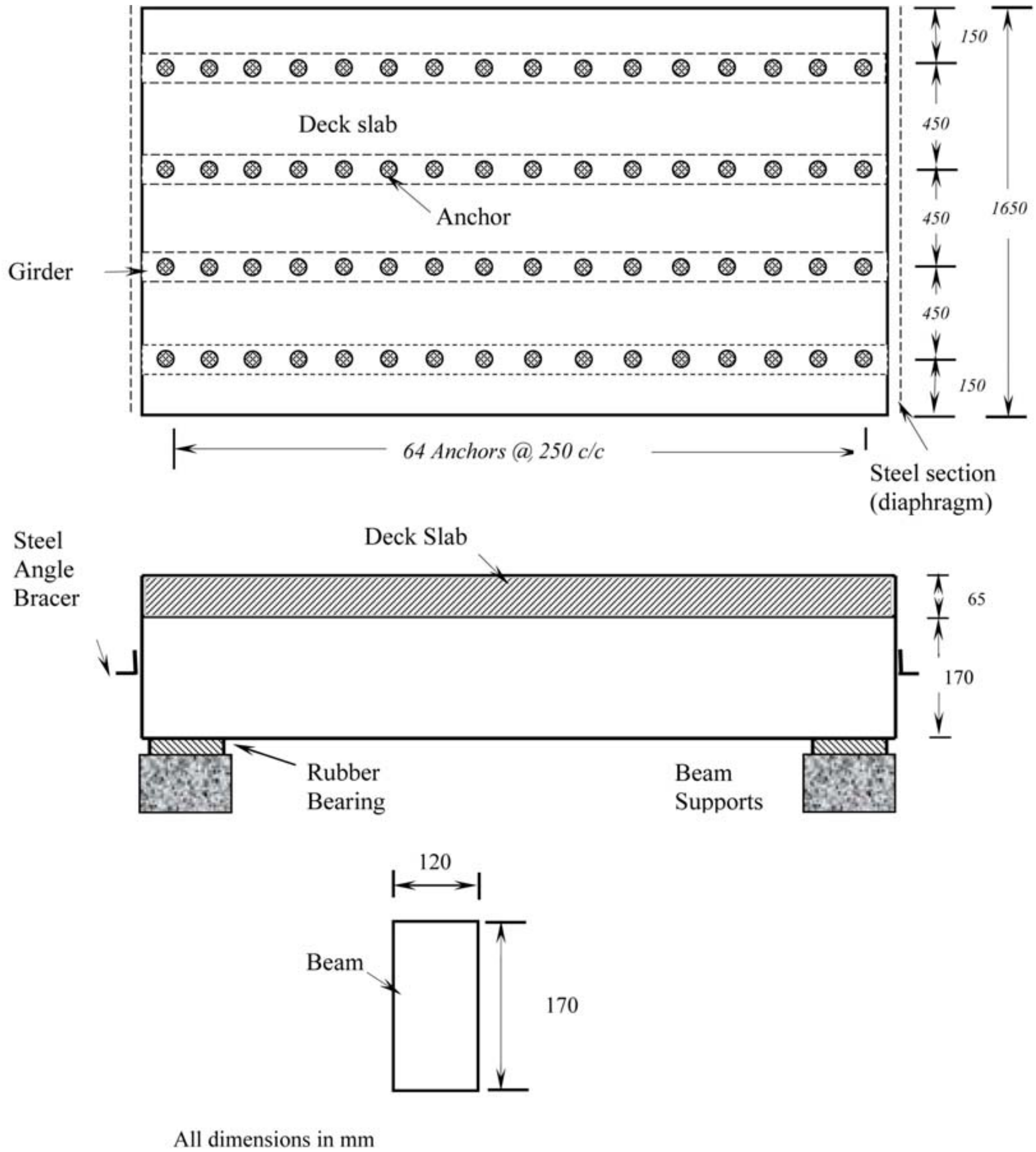

Fig. 6 Scaled bridge model

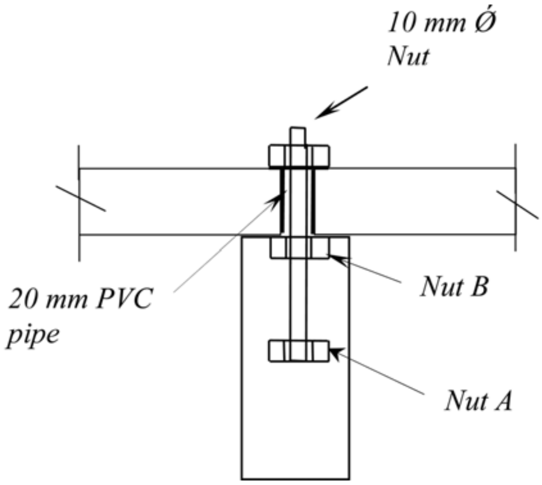

Fig. 7 Conncetion details

Fig. 8 Completed scaled model

4. Description of bridge model

Studies reported in literature on the behaviour of concrete-steel composites use simple single beam systems in which the transverse stiffness is assumed to be infinitely large (Thambiratnam and Brameld 1994). For studies related to dynamic-based condition assessment a bridge model where the transverse stiffness is finite would be appropriate. In this study the test model consisted of four 4200 mm long × 170 mm deep × 120 mm wide beams and a 4200 mm long × 1650 mm wide × 65 mm deep slab (Fig. 6). The beams were connected to the slab via 10mm diameter mild steel bolts cast into the beams at a spacing of 250 mm c/c (Fig. 7). The bolts acted as shear connectors for the model bridge. The connection was achieved by tightening each bolt by the same amount of torque, using a calibrated torque wrench. Damage was then introduced to the model by loosening selected bolts. The baseline scaled bridge model was established by applying a of 35 Nm torque to all bolts connecting the beams to the slab using a torque wrench. This model was used as the reference model for updating the theoretical modelling of partial composite action of the laboratory model.

The beams and the slab were normally reinforced. Transverse stability of the bridge model was provided by 50 mm × 50 mm equal angle steel sections bolted at the ends of girders as shown in Fig. 7 and Fig. 8. The beams were simply supported on 10 mm thick elastomeric bearings.

Target concrete compressive strengths for the slab and beams were 25 MPa and 35 MPa respectively. Fig. 8 shows the completed bridge model.

5. Description of finite element models

Two finite element models (FEM) of the bridge model were created, one assuming full composite action between the slab and the beams and the other assuming partial composite action between the beams and the slab. In both cases, the beams were modelled using 3D beam elements and the slab was modelled using shell elements in ADINA software (Fig. 9). For the case of full composite action coincident nodes were connected using rigid links while for the case of partial composite action, the connection between the slab and the beams was modelled using spring elements having axial stiffness and tangential stiffness parallel and perpendicular to the shear connector respectively. The bearings were represented by spring elements with rotational stiffness and translational stiffness in all three directions X, Y, Z as specified by the manufacturer.

Initial axial stiffness of the shear connectors was taken as the minimum of values obtained using Eq. (2) and Eq. (5). Following Eq. (2), and taking the Young's Modulus of steel to be 205 GPa, and the height, h, of the shear connector to be 65 mm, the initial axial stiffness is 2.48×10^8 N/m. Using Eq. (5), the height, e, of the shear connector to the centroid of the slab is 32.5 mm, giving an axial stiffness value of 7.08×10^8 N/m. Note that the tangential stiffness results from translation and rotation at the interface (Eq. (1)). Therefore two components of this stiffness must be estimated for

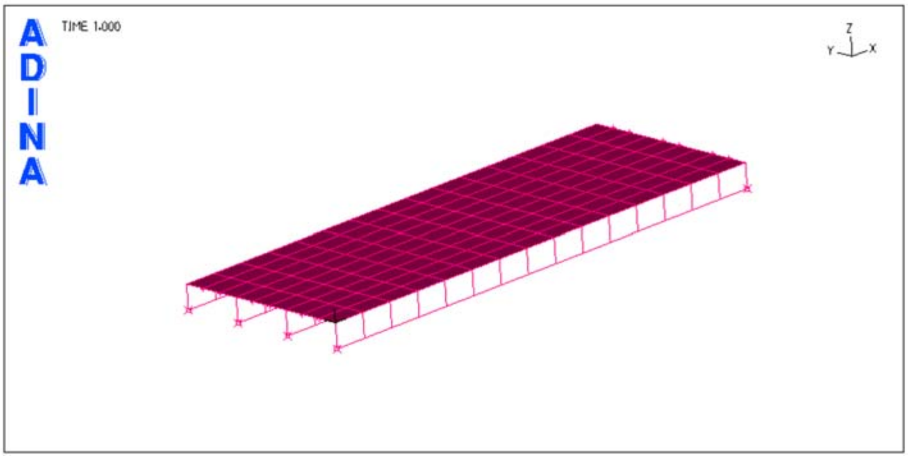

Fig. 9 FE model of the scaled bridge

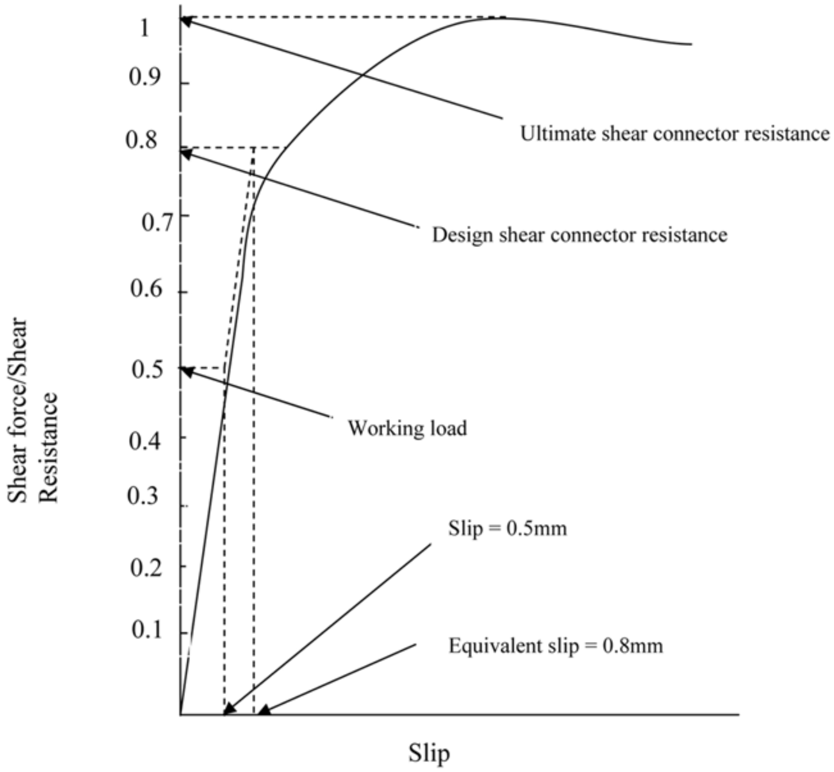

Fig. 10 Estiamtion of shear connector stifness

Table 1 FEM material properties

Property	Value
Modulus of elsaticity concrete beams	28E9 N/m^2
Modulus of elsaticity concrete beams	26E9 N/m^2
Density of concrete beams	2280 kg/m^3
Density of concrete slab	2007 kg/m^3

the spring element in ADINA, that is the translation stiffness and the rotational stiffness. The values of translational stiffness and rotational stiffness associated with the tangential stiffness were estimated as the secant stiffness at 50% of the ultimate load with an equivalent slip of 0.5 mm (Fig. 10). Observations by Wang (1998) from over 20 experimental results support this approach. Since the translation $u_{c1} - u_{c2}$ and the rotation ϕ are unknown, the initial translational stiffness was estimated assuming $\phi = 0$, in turn, the initial rotational stiffness was estimated assuming $u_{c1} - u_{c2} = 0$. For mild steel with an ultimate stress of 410 MPa, the translational stiffness component is 2×10^7 N/m, while the rotational stiffness is 2×10^7 Nm/rad.

Table 1 lists concrete properties used in the model. The material properties were determined experimentally.

6. Model updating

The dynamic properties of the model bridge were determined using vibration testing. Six units of Honeywell QA-700 force balance accelerometers, having resolution down to 10^{-5} m/sec^2 were used to capture accelerations. Broadband excitation was provided by an APS 400 long stroke electro-dynamic shaker. A PCB accelerometer was attached to the shaker to measure vertical acceleration and thus the excitation force on the bridge model. The measurement locations and the position of the shaker are shown in Fig. 11.

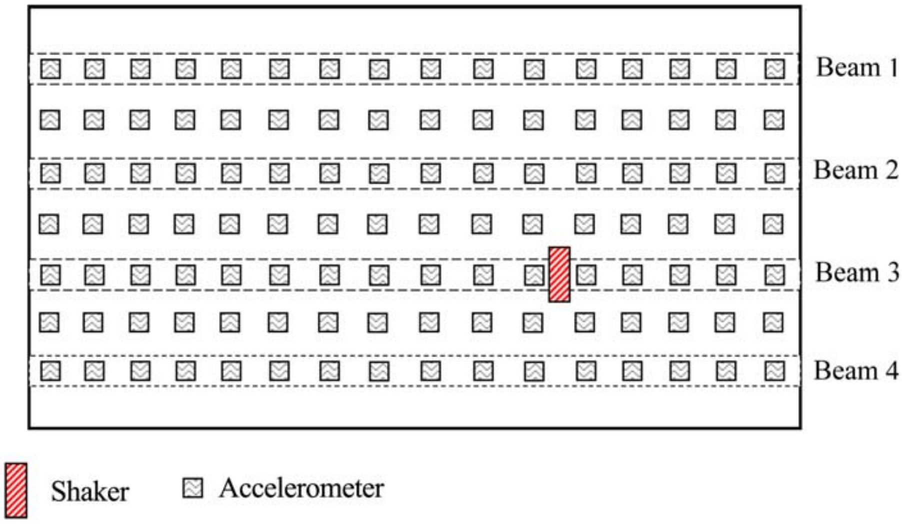

Fig. 11 Experimental modal analysis test arrangement

Table 2 Comparisons of analytical and experimental natural frequencies

Mode	Theoretical Frequency, Hz	Theoretical Frequency, Hz	Percentage Difference
1st Bending Mode	41.87	19.76	111.9
1st Torsional mode	49.12	29.01	69.3
2nd Bending mode	135.60	66.90	102.7
2nd Torsional mode	147.00	77.91	88.7
1st Transverse mode	104.60	85.94	21.

Table 3 Comparisons of analytical and experimental natural frequencies

Mode	Theoretical Frequency, Hz	Experimental Frequency, Hz	Percentage Difference
1st Bending Mode	19.76	19.71	0.25
1st Torsional mode	29.01	28.86	0.52
2nd Bending mode	66.90	67.69	-1.18
2nd Torsional mode	77.91	77.85	0.08
1st Transverse mode	85.94	86.51	-0.66

Table 4 Spring stiffness of bearings and shear connectors

Bearings		Shear Connectors	
Spring Property	Stiffness	Spring Property	Stiffness
X-Translation	$3*10^8$ N/m	*X*-Translation	$3*10^8$ N/m
Y-Translation	$3*10^8$ N/m	*Y*-Translation	$3*10^8$ N/m
Z-Translation	$3*10^8$ N/m	*Z*-Translation	$3*10^8$ N/m
X-Rotation	$1.8*10^6$ Nm/rad	*X*-Rotation	$1*10^5$ Nm/rad
Y-Rotation	$8*10^5$ Nm/rad	*Y*-Rotation	$7*10^8$ Nm/rad
Z-Rotation	$3*10^8$ Nm/rad	*Z*-Rotation	$3*10^8$ Nm/rad

Table 3 shows the first five measured natural frequencies and the corresponding mode shapes are shown in the first column of Table 6, under XO. FEM of the model bridge with partial composite action was manually fine-tuned, by adjusting the tangential and axial stiffness of the shear connectors, to match the experimental dynamic properties. The objective function was the frequency pair. A good agreement between the measured modes and theoretical modes was achieved as shown in Table 3. The final spring stiffness values for the baseline model are given in Table 4.

A comparison of natural frequencies was made between the updated model of the model bridge and the FEM model of the model bridge assuming full composite action. Table 2 shows the first 5 theoretical modes of the scaled bridge model assuming full composite action and partial composite action. The difference between the two models is obvious. Clearly the effect of partial connectivity between elements in concrete-concrete composite structures cannot be ignored in the modelling and analysis of these structures.

7. Damage assessment

A practical application of this work is the evaluation of the long-term performance of shear connectors using the calibrated model as a reference. The assumption is that a good characterisation of the materials properties and boundary conditions is carried out prior to re-calibration of the model. Damage assessment was carried out using experimental modal analysis and measurements were taken at positions shown in Fig. 11. Various damage scenarios were investigated to assess the sensitivity of the dynamic properties to changes in the shear stiffness. Damage was introduced to the bridge model by loosening selected shear connectors. The following damage cases investigated:

Case 1 (X1): This damage case simulated a light damage on the structure. Four shear connectors were loosened in the middle of the slab on two beams i.e., two on beam B2 and another two on B3 (Fig. 12), that is 6.25% of the shear connectors were damaged.

Case 2 (X2): For this case, eight shear connectors were loosened as shown in Fig. 13. This accounts for 12.5% of the shear connectors.

Case 3 (X3): For this case sixteen of shear connectors were loosened as shown in Fig. 14.

Case 4 (X4): For this case twenty four connectors were loosened as shown in Fig. 15.

Case 5 (X5): Case five is taken as the severe damage scenario. 75% of shear connectors are loosened (Fig. 16).

Table 5 shows a comparison of the first five measured natural frequencies for the five damage cases. The measured mode shapes for these cases are shown in Table 6. Generally the natural

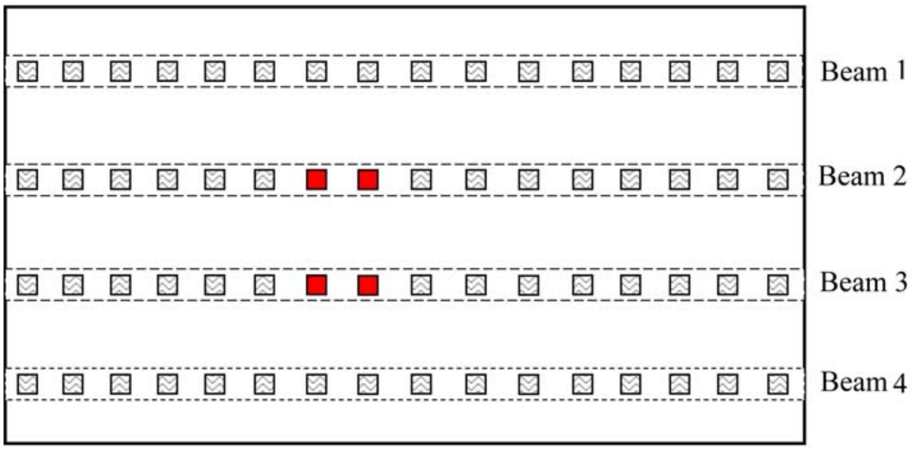

Fig. 12 Damage case 1

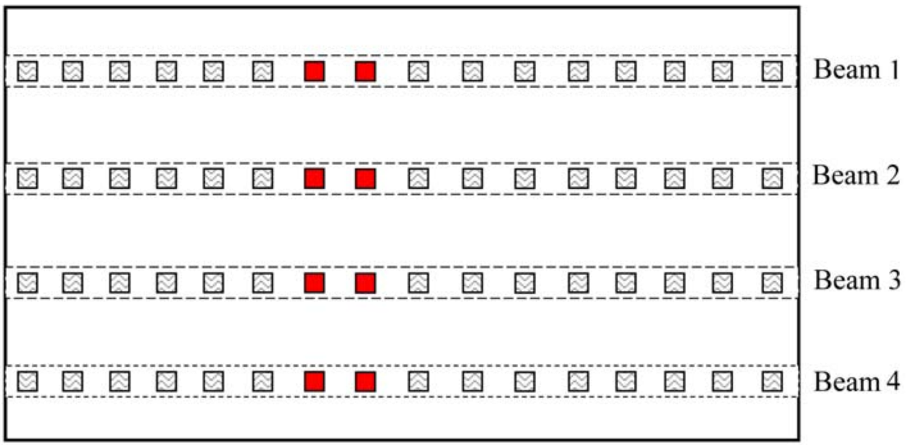

Fig. 13 Damage case 2

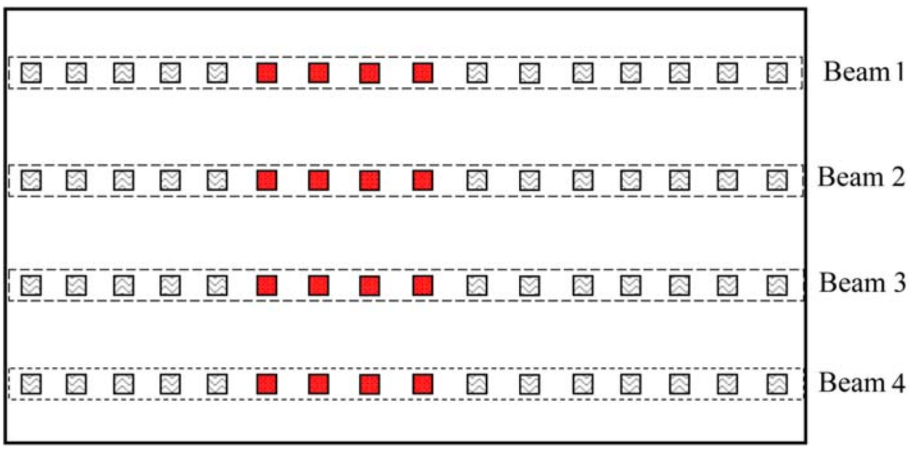

Fig. 14 Damage case 3

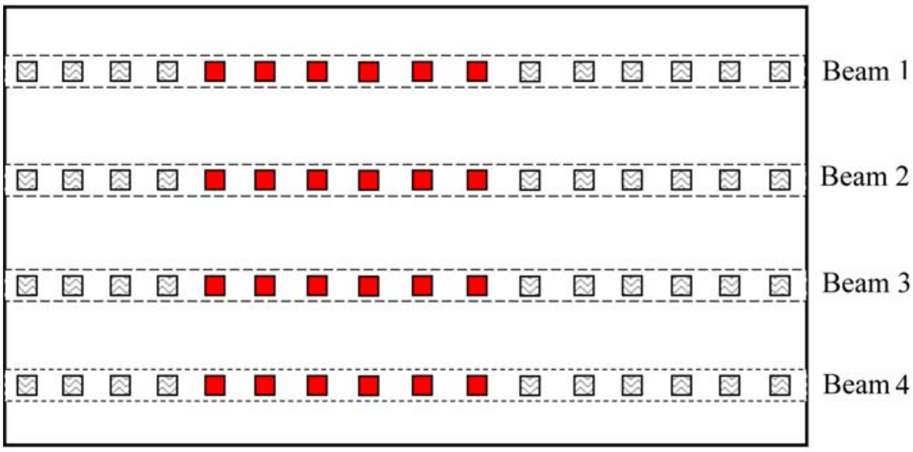

Fig. 15 Damage case 4

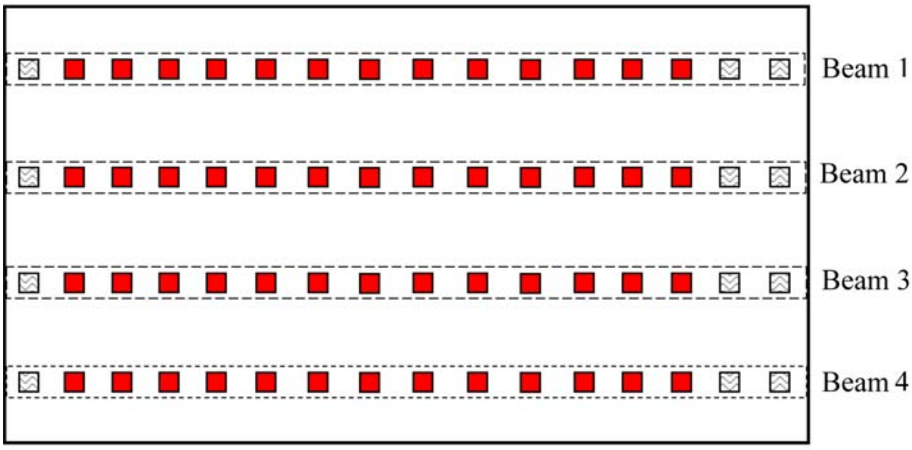

Fig. 16 Damage case 5

frequencies decrease with increasing level of damage as expected. The first bending mode is least sensitive to shear connector damage with a maximum percentage change of –8.6% for the most severe damage. The second bending and second torsion modes were most sensitive to damage with changes up to –25.3%.

8. Application

The modelling and calibration of concrete composite bridges described above was applied to a concrete composite highway bridge. The subject bridge is a multiple span bridge over the spillway of Van de Kloof Dam situated at the boarder between the Northern Cape and Free State Provinces in South Africa. Van der Kloof dam is a major dam on the Orange River (Fig. 17). The bridge over the spillway provides a vital link over the Orange River for tourism, the surrounding rural communities and in particular for the agriculture-oriented heavy vehicles. The bridge consists of

Table 5 Comparisons of analytical and experimental natural frequencies

Mode	Case	Analytical Frequency, Hz	Experimental Frequency, Hz	Percentage Difference
1st Bending Mode	X0	19.76	19.71	-0.3
	X1	19.75	19.59	-0.8
	X2	19.72	19.67	-0.3
	X3	19.57	19.30	-1.4
	X4	19.22	18.90	-1.7
	X5	15.88	18.01	+13.4
Torsional mode	X0	31.61	28.86	-8.7
	X1	31.01	27.93	-9.9
	X2	30.45	28.38	-6.8
	X3	29.67	27.91	-7.7
	X4	29.00	27.38	-5.5
	X5	27.62	25.65	-7.1
2nd Bending mode	X0	63.90	67.69	+5.8
	X1	63.73	66.47	+4.3
	X2	63.56	66.47	+4.5
	X3	63.02	60.13	-4.5
	X4	63.80	52.71	-17.4
	X5	48.41	50.54	+4.4
2nd Torsinal mode	X0	79.91	77.85	-2.6
	X1	79.84	75.36	-5.6
	X2	79.56	74.35	-6.4
	X3	79.32	71.77	-9.5
	X4	78.20	69.19	-11.5
	X5	75.41	59.57	-15.8
Transverse mode	X0	92.94	86.51	-6.9
	X1	92.00	83.93	-8.7
	X2	89.00	88.41	-5.9
	X3	78.78	86.71	+10.1
	X4	73.32	79.68	+8.7
	X5	148.90	67.62	-

fifteen simply supported 13 m spans between elastomeric bearings. Each span is made up of 9 pre-cast reinforced concrete beams and a cast in-situ reinforced concrete slab as shown in Fig. 18. Excessive vibrations experienced by motorists raised concerns about the bridge's structural integrity. Investigations indicated possible malfunction of elastomeric bearings, poor transverse stiffness and poor composite action between the pre-cast beams and cast in-situ slab.

Full scale dynamic testing was carried for system identification of the bridge. The results of dynamic testing were used to fine tune the FEM model of the bridge. The bridge was modelled in ADINA software using 3D beams elements and shell elements. The shear connectors were modelled using spring elements. Material properties were estimated from concrete cores taken from the bridge. In addition to the model that accounts for partial shear connection between the slab and the beams, an FEM assuming full composite action was created.

Table 7 shows the first five theoretical and measured natural frequencies. There is a difference of up to 59% between the measured natural frequencies and theoretical frequency of the bridge with

Table 6 Comparisons of experimental mode shapes for undamaged and damaged states

Mode	Damage Case			
	*X*0	*X*1	*X*3	*X*5
1st Bending	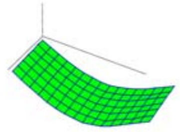	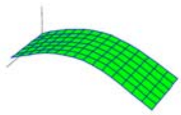	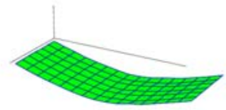	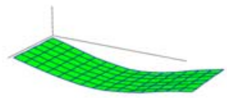
1st Torsion	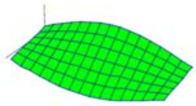	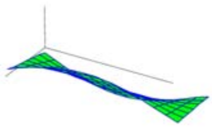		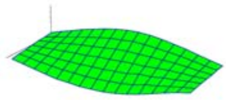
2nd Bending	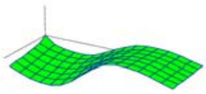	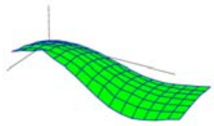	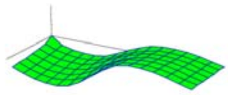	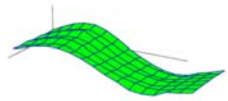
2nd Torsion	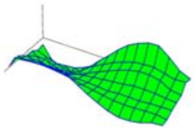	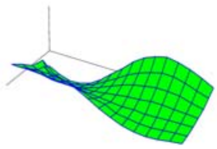	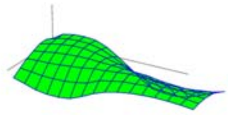	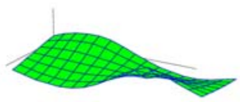
1st Transverse	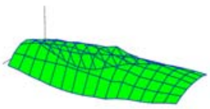	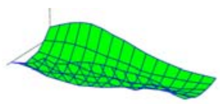	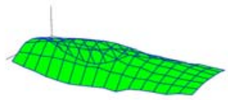	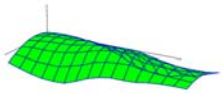

Fig. 17 Van der Kloof Dam

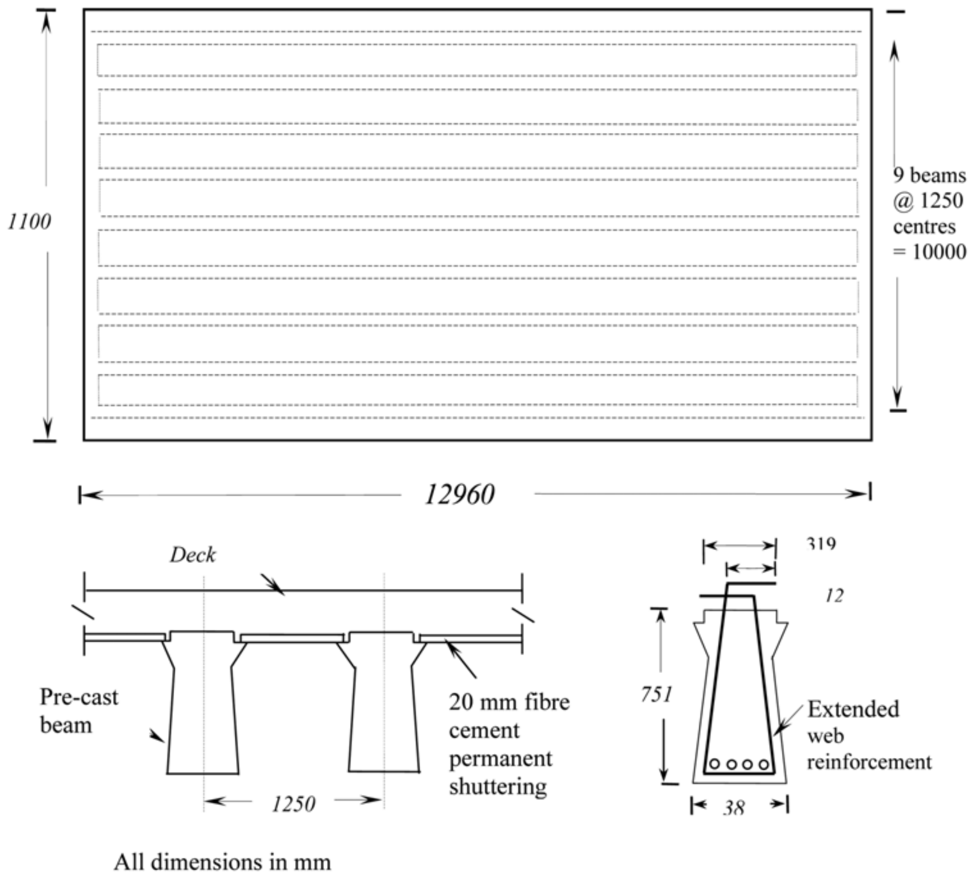

Fig. 18 Typical span details

Table 7 The first five identified frequencies of Van der Kloof Bridge: Pre-retrofitting

Van der Kloof Bridge (span 13 m)	Measured frequency(Hz)	Theoretical frequency (Hz)
1 bending	8.8	9.0
2 torsion	10.9	10.1
3 Transverse	13.1	12.8
4 Transverse	17.2	17.4
5 Transverse	22.9	23.9

full composite action. The updated model of the bridge with partial composite action shows good agreement with of the bridge measurements. This confirms that assuming full composite action between the slab and the beams would result in an incorrect model of the bridge leading to inappropriate rehabilitation interventions.

The updated bridge model was used as a basis for developing rehabilitation and retrofitting interventions. Retrofitting intervention at Van der Kloof Bridge included, replacement of all bearings with Freyssinet reinforced elastomeric bearing pads (300 × 152 × 22 mm), installation of two transverse beams at third points (45 MPa, self-compacting concrete) and installation of a 100 mm thick fully bonded concrete pavement (40 MPa concrete).

9. Conclusions

The condition assessment of concrete composite bridges requires appropriate modelling of the connection between concrete components. Vibration based testing and model updating show that FEM modelling of concrete-concrete composite structures should account for the partial composite action between the elements. Shear connector stiffness equations developed for steel-concrete composite structures provide reasonable initial values of stiffness values for concrete-concrete composites. The integration of modal analysis and model updating gives reliable FEM models for structural analysis and condition assessment.

References

Baska, K., Shunmugam, N.E. and Thevendran, V. (2002), "Finite element analysis of steel-concrete composite plate girder", *J. Struct. Eng.-ASCE*, **128**(9), 1158-1168.

Chen, S. (2008), "Discussion of long-term analysis of steel-concrete composite beams: FE modelling for effective width evaluation", *Eng. Struct.*, **30**(2), 1110-1121.

Clubley, S.K., Moy, S.S.J. and Xiao, R.Y. (2002), "Shear strength of steel-concrete-steel composite panels. Part I – testing and numerical modelling", *J. Constr. Steel Res.*, **59**(6), 781-794.

Dilena, M. and Morassi, A. (2009), "Vibrations of steel-composite beams with partially degraded connection and applications to damage detection", *J. Sound Vib.*, **320**(1-2), 101-124.

Faella, C., Martinelli, E. and Nigro, E. (2002), "Steel and concrete composite beams with flexible shear connection: "exact" analytical expression of the stiffness matrix and applications", *Comput. Struct.*, **80**, 1001-1009.

Faella, C., Martinelli, E. and Nigro, E. (2003), "Shear connection nonlinearity and deflections of steel-concrete composite beams: A simplified method", *J. Struct. Eng.-ASCE*, **129**(1), 12-20.

Fu, K.C. and Lu, F. (2003), "Nonlinear finite element analysis for highway bridge superstructures", *J. Bridge Eng.,* **8**(3), 173-179.

Johnson, R.P. (1994), *Composite Structures of Steel and Concrete* Vol. 1, 2nd Edition, Balckwell Scientific Publications Ltd., Oxford, UK.

Johnson, R.P. and May, I.M. (1975), "Partial interaction design of composite beams", *Struct. Eng.,* **53**(8), 305-311.

Macorini, L., Fragiacomo, M., Amadio, C. and Izzuddin, B.A. (2005), "Long-term analysis of steel-concrete composite beams: FE modelling for effective width evaluation", *Eng. Struct.*, **28**, 1110-1121.

Queiroz, F.D., Vellasco, P.C.G.S. and Nethercot, D.A. (2007), "Finite element modelling of composite beams with full and partial shear connection", *J. Constr. Steel Res.*, **63**(4), 505-521.

Ryall, M.J., Parke, G.A.R. and Harding, J.E. (2003), *Manual of Bridge Engineering*, Thomas Telford Publishing, London.

Seracino, R., Lee, C.T., Lim, T.C. and Lim, J.Y. (2004), "Partial interaction stresses in continuous composite beams under serviceability loads", *J. Constr. Steel Res.*, **60**(10), 1525-1523.

Taylor, H.P.J. (1998), "The precast concrete bridge beam - the last 50 years", *Struct. Eng.*, **76**, 407-414.

Smitha, M.Z., Li, Y. and Bulleit, W.M. (2011), "A method for evaluation of longitudinal joint connections of decked precast concrete girder bridges" *Struct. Eng. Mech.,* **40**(3), 297-313.

Thambiratnam, D.P. and Brameld, G.H. (1995), "Free vibration analysis of bridges", *Eng. Struct.*, **17**(10), 705-713.

Wang, A.J. (2011), “Numerical studies on shear connectors in push-out tests under elevated temperatures”, *Struct. Eng. Mech.,* **39**(3), 317-338.

Wang, A.J. and Chung, K.F. (2008), “Advanced finite element modelling of perforated composite beams with flexible shear connectors”, *Eng. Struct.*, **30**(10), 1000-1016.

Wang, Y.C. (1998), “Deflection of steel-concrete composite beams with partial shear interaction”, *J. Struct. Eng.-ASCE,* **124**(10), 1159-1165.

Wright, H.D. (1990), “The deformation of composite beams with discrete flexible connection”, *J. Constr. Steel Res.*, **15**(1-2), 49-64.

Xia, Y., Hao, H. and Deeks, A.J. (2007), “Dynamic assessment of shear connectors in slab-girder bridges”, *Eng. Struct.*, **29**(7), 1475-1486.

Xia Y, Hao, H., Deeks, A.J. and Zhu, X. (2008), “Condition assessment of shear connectors in slab-girder bridges via vibration measurements” *ASCE J. Bridge Eng.*, **13**(1), 43-54.